How to Cite:
Hatem, A. A. (2022). The effectiveness of nano-nickel oxide with manufactured plant extract and its properties on inhibiting the growth of some types of bacteria and fungi isolated from skin infections. *International Journal of Health Sciences*, *6*(S6), 9130–9151. https://doi.org/10.53730/ijhs.v6nS6.12410

The effectiveness of nano-nickel oxide with manufactured plant extract and its properties on inhibiting the growth of some types of bacteria and fungi isolated from skin infections

Asmaa Ahmed Hatem
Technical Medical Institute, Central Technical University, Baghdad, Iraq
*Corresponding author email: assma2222@mtu.edu.iq

***Abstract*---**Nickel oxide nanoparticles prepared in the first and second methods were synthesized and the properties of the solutions were shown. The XRD examination according to the MT values was at the drawing amount (111) 37.2, (200) 44.6, (220) 62.5 corresponding to the international measurements of Miller's Theta2 coefficient, while it was Sem examined the appearance of the shape of the rocky, cork, or spherical and spherical particles with a size of 10-25 nm, the TEM examination gave that nanoparticles with a size not exceeding 0.5-40 nm, the UV test of absorbance and permeability indicated that the solution is homogeneous and very light and the nanomaterial is at a value between 236-800 nm and indicates Energy gap values are 2.0-5.6 ev and that the material is semiconductive, which is evidence of the presence of nickel oxide. The Ftir test shows that the bonding sites for cobalt oxide are at 500-600, and the zeta Potential (ZP) test indicates that all solutions have very small values and that the material is not agglomerating and very light. Nano-solutions of the first method and the second method were prepared using different plants with gradient concentrations, namely, extract of Saffron (Crocus sativus L., turmeric Curcuma longa, Zingiber officinale and Cinnamomum verum. M (100%, 75%, 50%, 25%. It was found that the plant extract with the nickel oxide nanoparticle prepared in the second method, Green synthesis nanoparticles by plant extract, is more efficient than the nanoparticle prepared in the first method. It was found that the extract of nickel chloride with saffron and extract of nickel chloride with turmeric is more inhibiting than the extract of nickel chloride with ginger and nickel chloride with the students in the inhibition of isolates of Gram-positive bacteria S.aureus than on Gram-negative bacteria of Ps.aeruginosa in the diameters of the inhibition zone where they were Average diameters of bacterial inhibition for extracts of the four plants by the second method,

respectively 0.0,0.0,8,14,18,22,0.08,9,22,,,0.0,0.0,8,24,28,0.0,23,25 35)) As for the plant Cinnamomum verum, the average diameters of the inhibition zones were, respectively (0.0,0.0,0.0,60,,,12,12,20), as its effect was the lowest compared to other extracts, but the inhibition effect of S.aureus bacteria was the average 60mm which is the largest with high concentrations of the extract with nickel chloride and even more effective. The plant extracts of nickel chloride and ginger were more effective in inhibiting the growth of Ps. aeruginosa bacteria than on S. aureus bacteria. Ecoli bacteria. The results of the effect of nickel oxide solutions on the growth of fungi showed a significant inhibitory effect, indicating the absence of Trichophyton mentagrophytes, and that the nanomaterial also had an effect on the inhibition of fungal growth Candida albicans with a diameter of 13,10.23,35 mm respectively at 100% concentration.

***Keywords*---** aleo vera, Ps.aeruginosa, S. aureus, trichophyton mentagrophytes, candida albicans.

Introduction

Nanotechnology is the term used to cover the design, construction and functional use of structures with at least one distinct dimension measured in nanometers (Pal, Jana, Manna, Mohanta, & Manavalan, 2011). The physical (top-to-bottom) and chemical (bottom-up) approaches are usually expensive and costly processes, not environmentally friendly and have toxic effects (Seabra & Durán, 2015). Modern methods have been introduced to the fabrication made of high-quality nanomaterials. This can be achieved by a simple green synthesis compared to conventional micro-synthetic nanoparticles. It would help to eliminate difficult processing conditions, by allowing the synthesis at physiological pH, temperature, pressure and low cost (Bardají et al., 2016). The skin is the first mechanical barrier that prevents pathogens and foreign materials from penetrating it and causing infection (Cianci, Slade Jr, Sato, & Faulkner, 2013). S. aureus is a Gram-positive bacterium.

It has a spherical shape and a diameter of 1.0-0.7 microns. It appears under the microscope in irregular clusters and may appear singly or in the form of a short assembled chain that is non-motile and does not form spores (Al-Nashi & Al-Mansoori, 2017). It is one of the most important species from a medical point of view and it can be distinguished from other species by its ability to produce the plasma clotting enzyme, which is one of the main virulence factors in these bacteria (Al-Salmi, 2014). Ps. aeruginosa, a Gram-negative bacterium with dimensions of about 0.6 x 2 microns, is not sporangia-forming, transmitted by a polar flagellum that forms a living antenna. It is an opportunistic pathogen that causes 10-20% of hospital infections. This bacterium is considered one of the very dangerous bacterial species because the infections caused by it are difficult to treat (AL-Hilli, 2000) as it is characterized by its multi-resistance to life antibiotics. Also, it becomes a strong pathogen whenever it enters the areas devoid of defenses, as in the case of skin and mucous membrane ruptures, helped by their various virulence factors, such as the production of hemolytic enzymes

(Haemolysin) and proteinase, as well as the production of many exotoxins that are equivalent in effectiveness to Diphtheria toxin(Behzadi, Baráth, & Gajdács, 2021). This bacterium is the most common cause of burn injuries (Bassetti, Vena, Croxatto, Righi, & Guery, 2018), and it was found that about 25% of burn patients hospitalized for treatment are infected with this bacterium. Microns arranged singly or in pairs, moving by circumferential flagella, or they are immobile, consuming most carbohydrates, forming acid with gas, and its colonies appear dry and pink on the medium of the Maconkey for fermentation of lactose sugar. Two types of exotoxins are produced, the first is heat labile, and the other is heat stable, and causes cases of summer diarrhea in infants. It also causes infections of wounds and burns as a result of its movement from its natural place of existence, which is the intestines, to other areas of the body, in addition to being considered the first pathogen that infects the urinary tract, causing urinary tract infections of varying severity.

Dermatophyte T. mentayrophyte is characterized by flat, domed, white colonies with copious conidia and the edges of the colonies are semi-radial. Small conidia often appear in clusters and arranged on the sides of the hyphae (Ernest Jawetz, Adelberg, & Melnick, 1987). This fungus is the main cause of tinea pedis (Tineapedis) as well as body tinea. This type is the main cause of tinea capitis, tinea auris, tinea auris, and tinea mannm (Alteras, Aryeli, & Feuerman, 1980). As for Candida albicans, it is the most common type that infects the skin in different areas of the human body. Its cells are characterized by their oval shape, and their diameters range between 10-6 x 6-3.5 microns. It is in the form of single cells or in the form of pseudophypha in the tissues of the host as it forms the germ tube, which is the preparatory stage for the invasion of host tissues (SOLL & BEDELL, 1978). The external parts of the body, such as the skin, hair and nails, are exposed to infection with this yeast because they possess two types of enzymes, which are proteinase and keratinase, which help them to infect the outer layer of the keratinized (Negi, Tsuboi, Matsui, & Ogawa, 1984). The infection occurs in the form of vesicles in the armpit, under the breasts and between the fingers then turns into dark red spots accompanied by itching and burning with crusting in the area (E Jawetz & Melnick, 1980).

Materials and Methods of Preparation

The method of work was selected according to the source (Srivastava, N., & Srivastava, P. C. 2010). The prepared solutions are placed by mixing method according to molarity of 1M for each solution to be mixed according to the table below: NT4: nickel nitrate + sodium hydroxide. NT3: nickel chloride + Saffron plant (Crocus sativus L.). NT6: nickel nitrate + Saffron plant (Crocus sativus L.). NT7: nickel chloride + Curcuma longa plant. NT8: nickel chloride + Zingiber officinale NT5: nickel chloride + Cinnamomum verum.

Preparation of nanoscale nickel oxide NiO The first method NANOPARTICAL STRACTUR Nickel nitrate with sodium hydroxide

1 M molar solutions are prepared from a solution of nickel chloride (NiCl2 6H2O). 1000\ The required volume M = weight \ 236.42 x 1000\ 100 M = 23.6 g Then 100 ml of 4% sodium hydroxide solution is added to get nickel oxide.

Preparation of nano-solutions: nickel oxide (NiO), the second method GREEN NANPRACTICAL

Nickel nitrate solution with saffron was prepared with saffron solution (Joseph, B 2012).

Materials

Saffron was taken 1 gm weight + 100 ml distilled water and then added to the nickel chloride solution. Nickel chloride with turmeric (Archana, Nandish, Savalagi, & Alagawadi, 2013) was used for turmeric solution(Rahman & Noor, 2012).

Materials

- Turmeric of 1 gm weight + 100 ml of distilled water was added to the nickel chloride solution.
- Nickel chloride with ginger preparation of ginger solution (Ahmed, Aly, Abd El-Baky, & Waly, 2020). Ginger with 1 gm weight + 100 ml of distilled water was added to the nickel chloride solution.
- Nickel chloride with the scholars (Rahman & Noor, 2012) of the Preparation of the scholars' solution (Al-Ani & Al-Qattan, 2017).

The students took 1 g weight + 100 ml of distilled water and then added it to the nickel chloride solution Bacterial Pathogen Isolates. The swab was taken with a sterile swab (Swab) and transferred to the hospital laboratory and initially cultured on blood agar medium in MacConkey agar medium. EMB agar was incubated at 37oC for 48-24 hours. The bacteria were identified morphologically, bacteriologically and biochemically.

Preparation of culture media for isolates of fungal pathogens

Identification of Fungi and pathogenic yeast: Fungi and yeasts were diagnosed and isolated based on the phenotypic characteristics of the colony, such as the shape, color, diameter, and height of the colony, as well as the microscopic characteristics such as the shape, size and color of conidia. In addition, some chemical tests were adopted in the diagnosis using the following sources (Feliciano Guzmán, 2016).

Culture of Specimens

After a direct microscopic examination of the samples, a portion of the sample was taken and planted on the surface of a sterile glass dish containing SDA Sabouroud Dextrose Agar Medium to prevent the growth of bacteria and sauropod fungi (non-pathogenic) and thymine and yeast extract were added to SDA to promote the growth of some types of filamentous dermatophytes and incubated. Cultures were at 28-30ºC for filamentous fungi and at 37ºC for yeasts. Sabauroud Dextrose Agar Medium (SDA) was prepared according to Emmons (1974)by dissolving 40 gm of dextrose, 10 gm of peptone, 20 gm of agar and 0.05 gm of the antibiotic chloramphenicol, then the volume reached to 1000 ml using distilled

water placing the mixture in clean and sterilized glass flask in a sterilizer at a temperature of 121°C and a pressure of 15 pounds/ing2 for 20 minutes. After sterilization, chlorine was added. This medium was used before (Al-Mousawi, 1997) to isolate opportunistic fungi and Emmons sabauroud Dextrose Agar Mediam (ESDA). This medium was prepared according to Eirmis (1980) by dissolving 20 gm dextrose, 10 gm peptone, 20 gm agar and 0.05 gm of the antibiotic Chloramphenicol, which was added after sterilization and then the volume was completed to 1000 ml of distilled water and then sterilize the medium with autoclave at a temperature of 121 °C and a pressure of 15 pounds / ing2 for a period of 20 minutes. Germ tube test This test was carried out according to Collee, Fraser, Marmion, and Simmons (1996)which is a test to differentiate between the species belonging to the genus Candida Spp. . This is done by inoculating 0.5 ml of sheep serum with inoculum from colonies of this genus and incubated at o37 C for 2-3 hours. One side of the cell when part of the colonies was incubated with sheep serum for 2-3 hours at a temperature of 37°C.

Results and Discussions

Assays of the nickel oxide nanomaterial

The tests were carried out to ensure the presence of nanoparticles in the following solutions of the nickel oxide compound (Pal et al, 2011). (Srivastava, N., & Srivastava, P. C. 2010) 1. XRD examination is a test that shows how it is conducted on the formation of nickel oxide by matching the results with international specifications and matching charts. It is the most important examination and the first in which the nanomaterial is tested (Jalill, Raghad, Nuaman, & Abd, 2016). The XRD assay is a basic test and the first to test the presence or absence of nanomaterials. Table (1) shows that the results of the examination are close to the international measurements of Miller's coefficient and indicates the presence of nickel oxide in the sample of the first method and the sample of the second method. Through the graph of the nickel compound, Figure (1) shows the presence of the nanomaterials 37.02 (111, 44.6 200)), 62.5 (220) in each of the materials NT3, NT5, NT6, NT6, NT7, NT8 and NT4. The results are consistent with the graph of the first method and the second method with the international measurements of Miller's coefficient 2, Theta deg). It was found in a study by the researcher (Abd, A., Ali, R., & Hussein, A. 2016),

Table 1
The values of Miller's treatment (MT) for nickel oxide in comparison to international measurements

The compound nickel oxide	international measurements	NT3(2 theta (deg)	NT4(2 theta (deg)	NT5(2 theta (deg)	NT6(2 theta (deg)	NT7(2 theta (deg)	NT8(2 theta (deg)
Ni(OH)2 Nio2 (001)	19.36	18.65	19.15	18.65	19	18.6	18.9
Nio (111)	37.02	35.35	38.95	38.5	37.35	38.55	35.85
Ni(OH)2 Ni (100)	39.36	35.35	38.95	38.5	37.35	38.55	35.85
Ni(OH)2 (101)	40		38.95				

Nio (200)	42.98		42.6	43.3	41.75	41.6	
Ni(OH)2 Ni2o3 (100)	43.94	44.7	42,6	43,3		43.45	
Nio (200)	44.6	44.7		44.75		44.8	45.1
Nio (220)	62.5	62.6	62.45		61.15	60.3	
Ni (04.-0.850)	78.79	74.3		74	73.95	74,8	

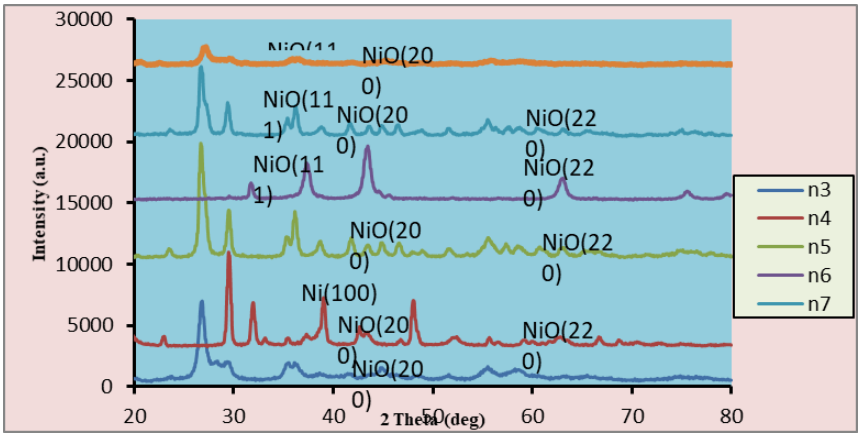

Figure 1. A graph of the XRD results for the first method NT4 for nickel oxide and the second method NT3,NT5, NT6, NT6, NT7, NT8 for nickel oxide

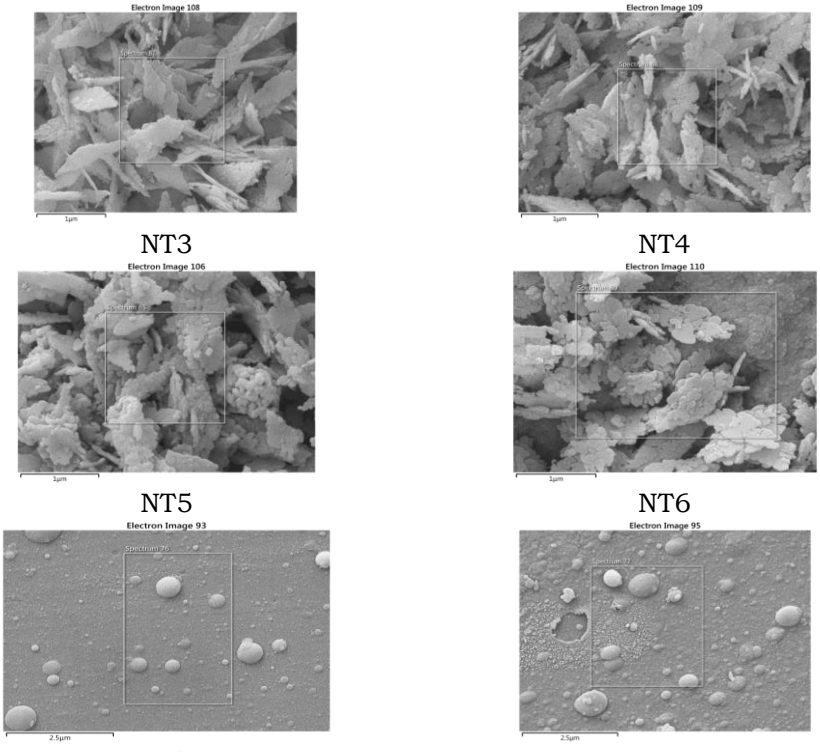

Figure 2. The results of the sem examination, the first method nt4 for nickel oxide and the second method nt3, nt5, nt6, nt6, nt7, nt8 for nickel oxide

Figure 2. is the NT3 material that is deposited on the glass, where the background appears black. Rock or cork particles shape almost spherical and semi-spherical with dimensions not exceeding 400-500 nm at the scale of the drawing and these particles appear with the dimensions of drawing size 25 nm smaller than 100 nm. As for the figure No. (17) NT4, the particle appears in the form of a shell or semi-shell with a smaller size of 10 nm, and it may aggregate to a size of up to 300 nm for nanoparticles. Figures No. (18, 19) NT6, NT5 are images that purify the 20nm particle, while Figure NT7 and NT8 show the spherical particles like gravel, the smallest size is 10 nm, and they may aggregate to a size of 2.5 μm for nanoparticles (Jalill et al., 2016).

TEM test is a test for finding the shape and size of a nanoparticle before deposition.

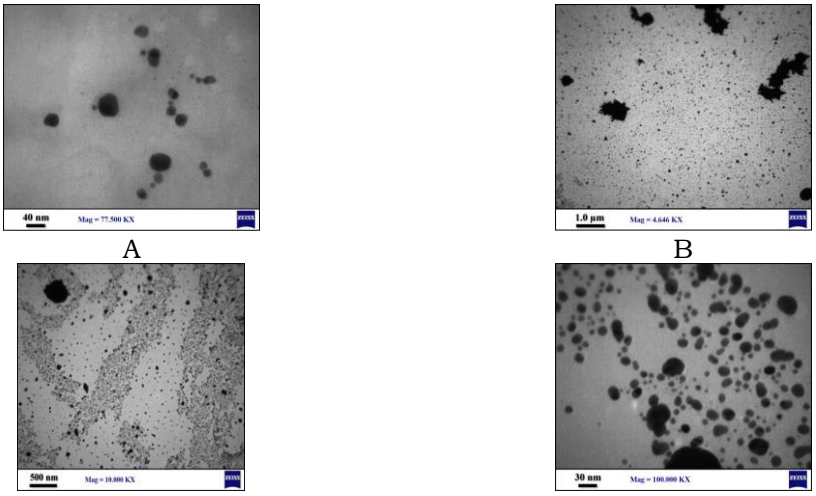

Figure 3. TEM Nickel oxide solution NT4 The first method NT3 The second method

It was noticed from Figure (3) NT3 that the nanoparticles in the solution, the largest image scale A was 1.5μm. They were single and large spherical bodies connected to each other and according to the scale in the image B shows the nanoparticle whose drawing scale was 40nm. It is noted that different sizes of nanoparticles do not exceed Sizes range from 0.5-40 nm. It is noticed from Figure No. (23) NT4 that the nanoparticles in the solution, the largest image scale A was 500 nm. They are single and large spherical bodies connected to each other, and according to the scale in Image B, the drawing scale was 30 nm. It is noted that different sizes of nanoparticles do not exceed sizes ranging from 0.5- 30 nm.

A B

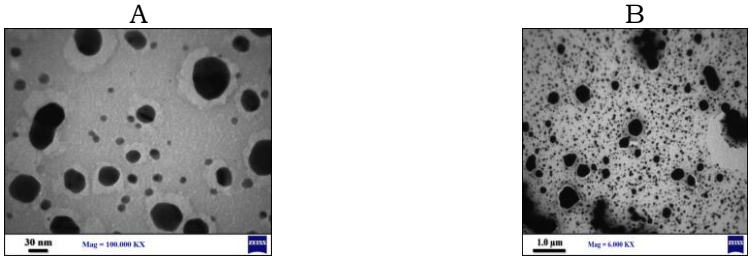

A B

Figure 4. TEM Nickel oxide solution NT6 The second method NT5 The second method

It was observed from Figure No. (4) NT5 that the nanoparticles in the solution were the largest image scale A was 1.0µm. They were single and large spherical bodies connected to each other, and according to the scale in Image B, the drawing scale was 30nm. It was noted that different sizes of nanoparticles did not exceed sizes ranging from 0.5 -30 nm. It is noted from Figure No. (25) NT6 that the nanoparticles in the solution, the largest image scale A was 250nm. They were single and large spherical objects connected to each other, and according to the scale in Image B, the drawing scale was 30nm. It was noted that different sizes of nanoparticles did not exceed sizes ranging from 0.5- 30 nm.

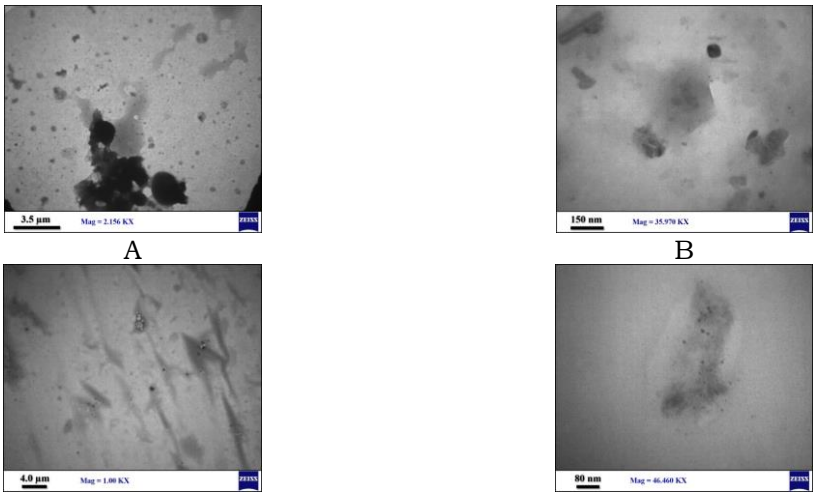

A B

A B

Figure 5. TEM Nickel oxide solution NT8 The second method NT7 The second method

It was noted from Figure (5) NT7 that the nanoparticles in the solution, the largest image scale A was 3.5µm. They were single and large spherical bodies connected to each other, and according to the scale in the image B, which was 150nm, it was noted that different sizes of nanoparticles did not exceed sizes ranging from 0.5 -1 nm. It is noticed from Figure (5) NT8 that the nanoparticles in the solution, the largest image scale A was 4.0µm, they are single and large spherical bodies connected to each other, and according to the scale in the image B, the drawing scale was 80 nm. 0.5-15 nm.

UV test is to test the transmittance and absorption coefficient and determine the energy gap.

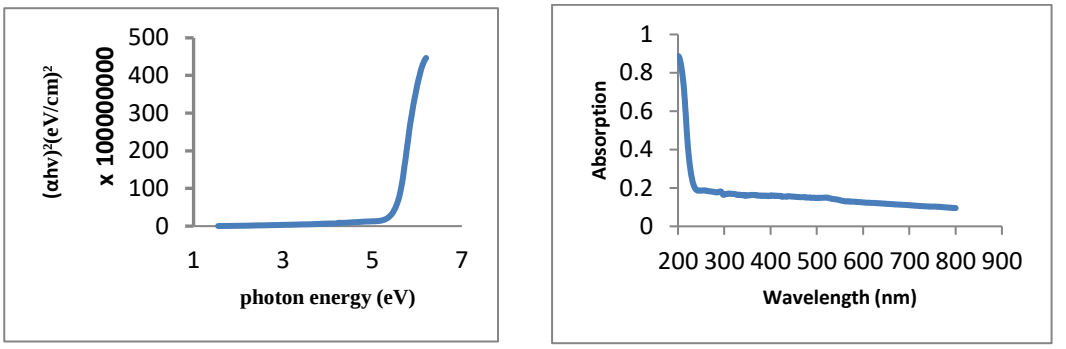

Figure 6. UV, energy and absorption gap of nickel oxide NT3 solution, second method

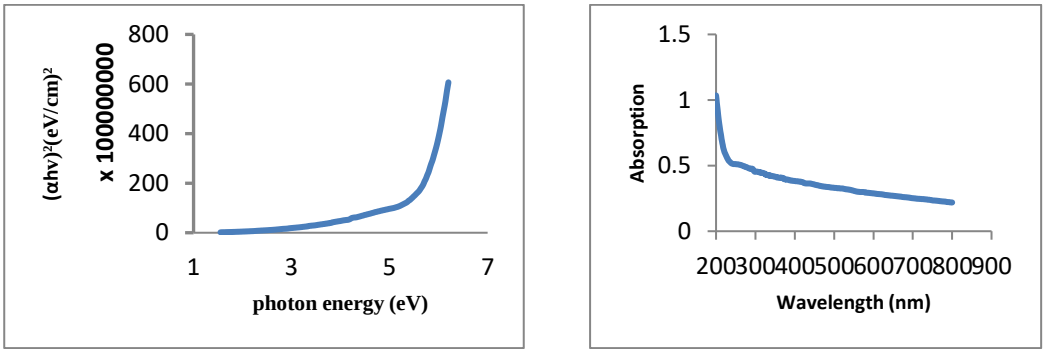

Figure 7. UV and the energy and absorption gap of the nickel oxide solution NT4 The first method

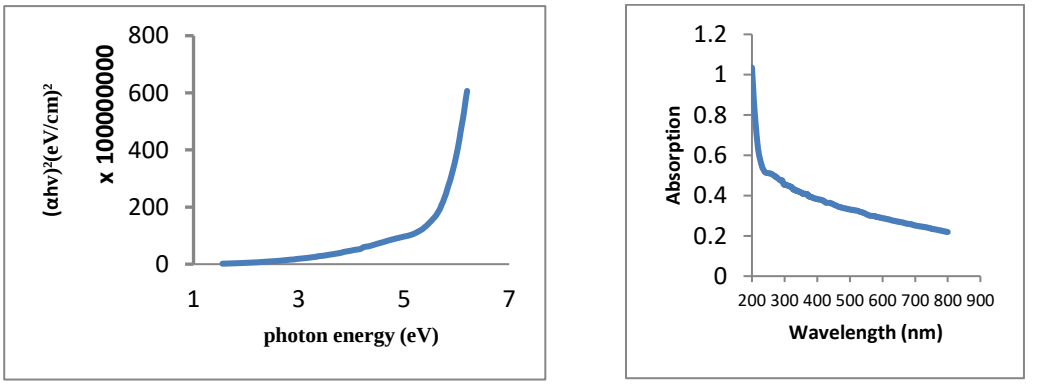

Figure 8. UV and the energy and absorption gap of the NT5 nickel oxide solution the second method.

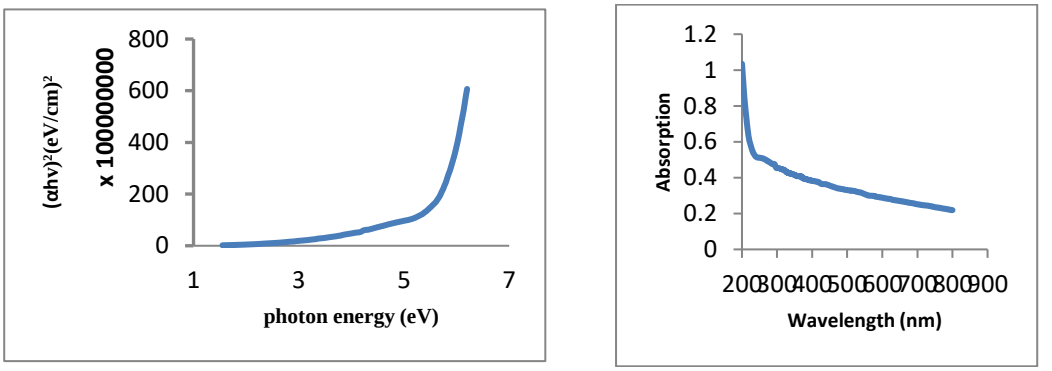

Figure 9. UV, energy and absorption gap of nickel oxide NT6 solution, second method

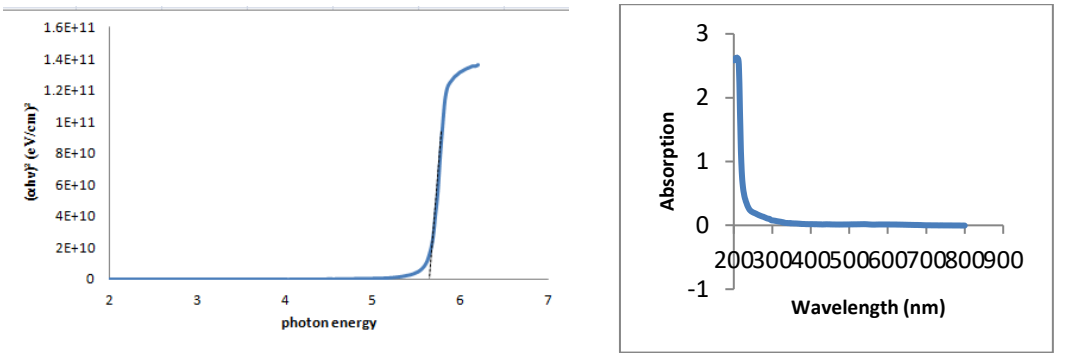

Figure 10. UV and the energy and absorption gap of the NT7 nickel oxide solution The second method

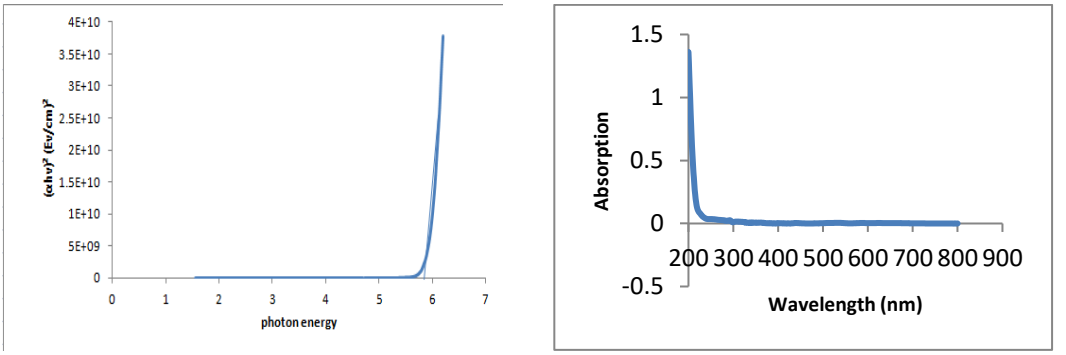

Figure 10. UV and the energy and absorption gap of the NT8 nickel oxide solution the second method

Figure No. (6) shows the UV graph A of the absorbance of the NT4 nickel oxide solution, the first method deposited on glass. It is noted that the material has a high absorbance at 200 - 236 nm, and it is noted that at more than 236 nm it has a very low absorbance (high transmittance), which is the range from 236 - 800 nm, and the graph indicates that the material with high transmittance behaves like a window (it is an optical property that means The material is transparent in the visual sense. Translucent means that the solution is very well homogeneous

and light. This is due to the complete homogeneity of the material and the deviation of absorption towards short waves, which indicates the formation of very small nanoparticles. As for Figure No. (6) UV, graph B is the energy gap, which is important in electronic transitions, and it is an optical property, so if the material is transparent or opaque (opaque). The importance of the energy gap is that the curve is in contact with the x-axis and cuts it by a point. This point is an angle called the energy gap of high value. It is semiconductive like metal oxides in the drawing. The value of the energy gap is 3.5 eV, which is a semiconductor material and it achieves the oxide of the nanomaterial. As for Figure No. (7,8,9,10,11) UV Absorption and Energy Gap Cobalt Oxide Solution NT3,NT5,NT6,NT7,NT8 The second method Graph A indicates that the material is transparent with high permeability and very little absorption at the range 236-800nm.

The solution is homogeneous and very light, and this is due to the complete homogeneity of the material and the deviation of the absorbance towards the short waves, which indicates the formation of very small nanoparticles. As for Figure (7), Chart B. The energy gap is of high value, as it is a semiconductor like metal oxides. In the NT3 sample graph, the energy gap value is 4.3 eV, which is a semiconductor material that realizes the oxide of the nanomaterials. As for Figure No. (8) in the graph of the sample NT5, the value of the energy gap is 2.2 eV, which is a semiconducting material that achieves the oxide of the nanomaterials. As in Figure No. (9) the graph of the NT6 sample, the value of the energy gap is 2.2 eV, which is a semiconducting material that achieves the oxide of the nanomaterials. As for Figure No. (10) in the graph of the NT7 sample, the value of the energy gap is 5.3 ev, which is a semiconducting material that achieves the oxide of the nanomaterials. As in Figure No. (11) the graph of the sample NT8, the value of the energy gap is 5.6 ev, which is a semiconducting material that achieves the oxide of the nanomaterials (Abd, A., 2016).

The FT-IR test is a test to check the effective chemical bonds and its identification is the analysis of the effective bonds

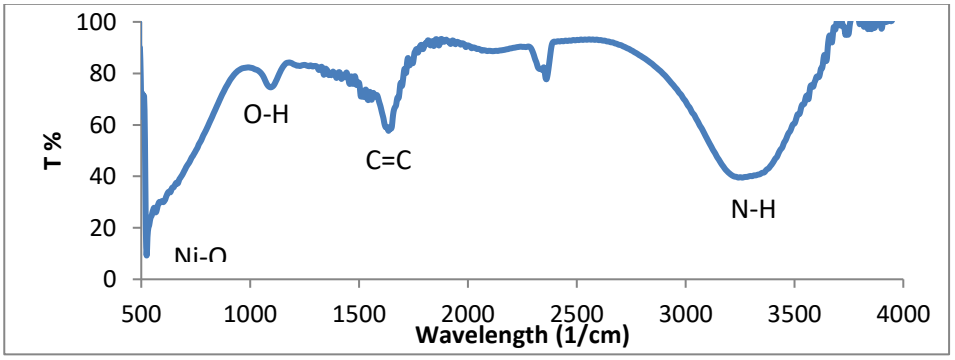

Figure 12. FT-IR Nickel Oxide NT3 solution, second method

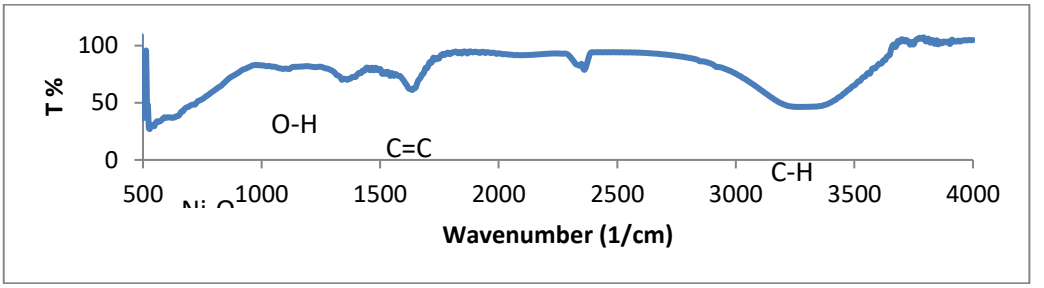

Figure 13. FT-IR Nickel Oxide NT4 solution, second method

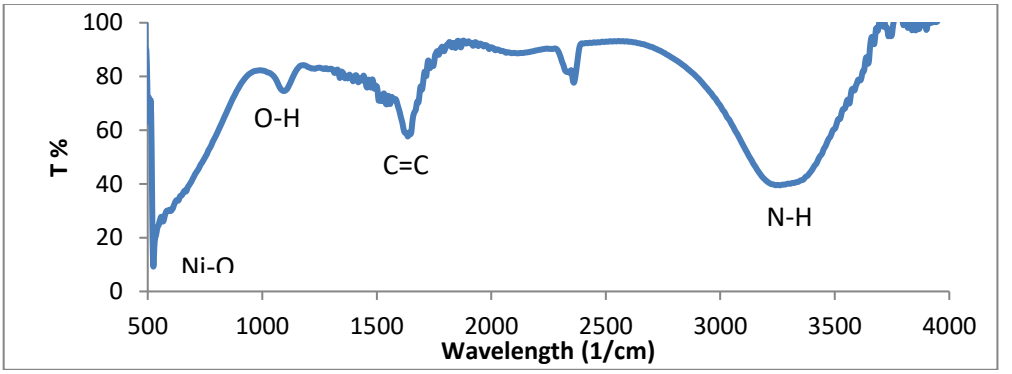

Figure 14. FT-IR Nickel Oxide NT5 solution, second method

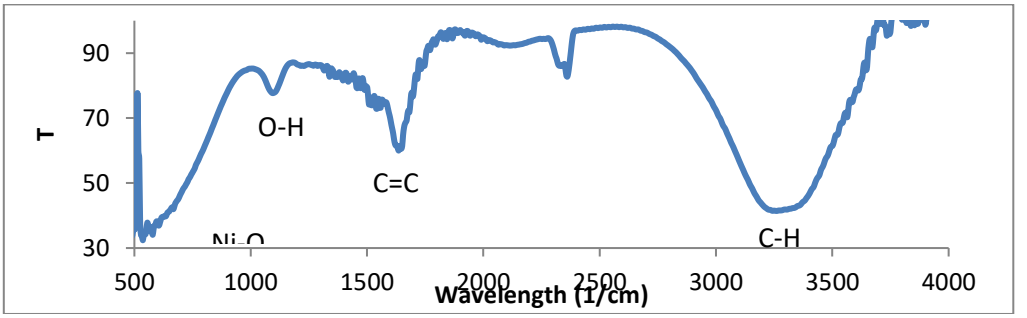

Figure 15. FT-IR Nickel Oxide NT6 solution, second method

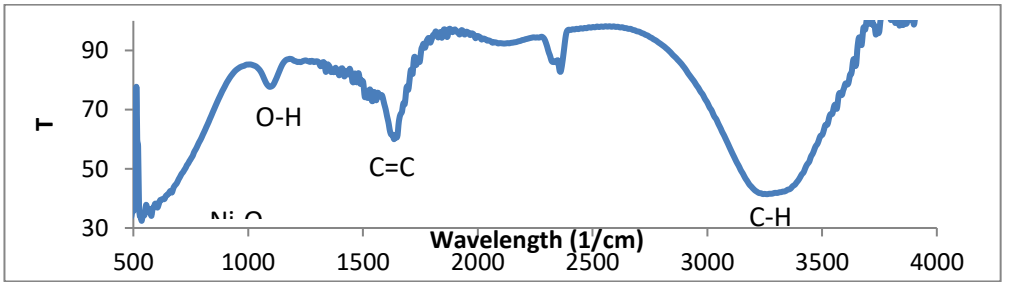

Figure 16. FT-IR Nickel Oxide NT7 solution, second method

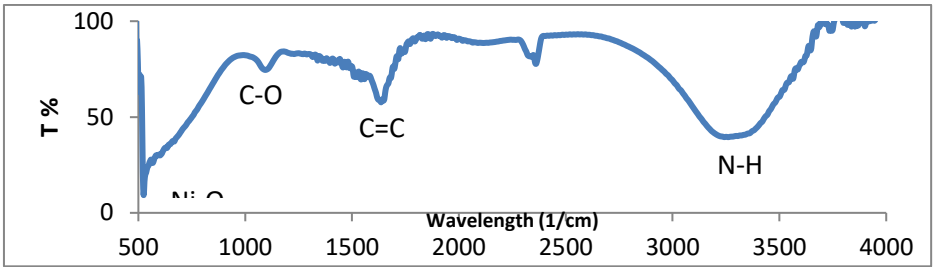

Figure 17. FT-IR Nickel Oxide NT8 solution, second method

It is observed from the figure figure No. (12,14,15,16,17) FT-IR nickel oxide solution for nanosolutions of plant extract NT3, NT5, NT6, NT7, NT8 The second method and from Figure (13) the graphic image No. NT4 The first method: The locations of the metal oxide Ni-O bonds are at 500-600, and it is noted that there is a wavelength of 1210 that is at the C-O bond level, it may be 2400 O-H bonds, 3300 N-H bonds and this is according to the vibration table in the source (Shuihab, A., 2018). The presence of an N-H bond is an amino acid bond for a type of protein. The importance of the effective bonds maintains the dimensions between substances and maintains volumes and does not cause agglomeration. The presence of N-H confirms its presence on the plant substance in the solution. The presence of the plant is important in the process of oxidation, reduction and color transformation in the solution. It has a major role in encapsulating nanoparticles so that no agglomeration of the material occurs, as in Figure No. 17, and it is noticed that whenever the nanoparticles dilute the particles with a strong charge of high attraction and repulsion, the process of agglomeration does not occur and the material descends when preparing at the bottom of the pot according to the table for values of wavelength source (Enders, North, Fensore, Velez-Alvarez, & Allen, 2021).

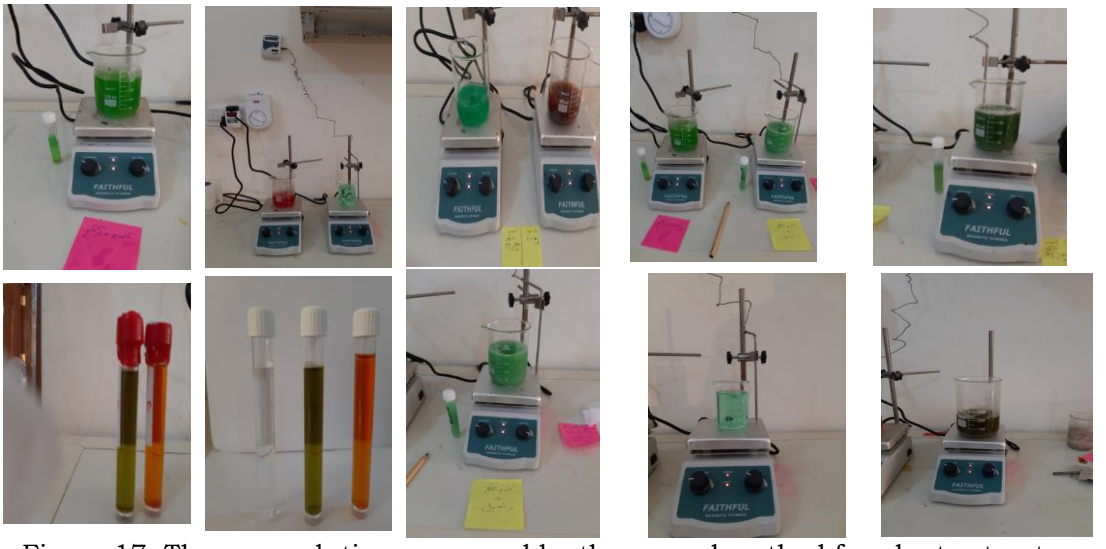

Figure 17. The nanosolutions prepared by the second method for plant extracts showing that the presence of color is evidence of the formation of nanoparticles in the solutions

Zeta Potential Assay

It is the determination of the particle size and surface charge of the dynamic light scattering zp factor potential (Malvern Instruments, L. 2012).

Peak No.	Zeta Potential	Electrophoretic Mobility
NT4	0.9 mv	0.000007 cm2 / vs
NT3	-43.6 mv	-0.000339 cm2/ vs
NT7	-4.9 mv	-0.000038 cm2/vs
NT6	-17.8 mv	-0.000138 cm2/vs
NT8	-25.1mv	-0.000195 cm2/vs

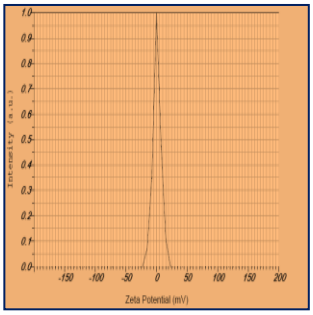

NT4

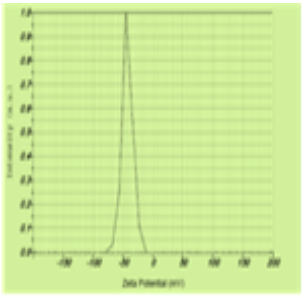

NT7

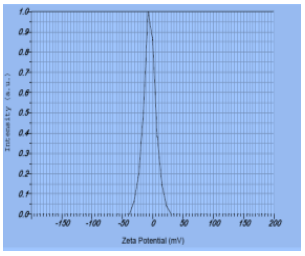

NT8

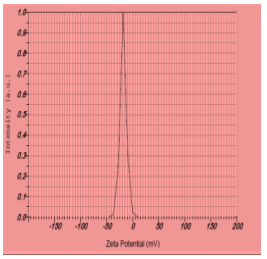

NT3

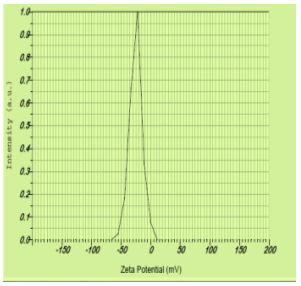

NT6

Figure 17. The results of Zeta Potential for cobalt oxide solutions, the first method NT4 and the second method NT7, NT8, NT6

It was noticed from the results of the Zeta examination, it was noted that there was an amount of positive incompatible value, which is the evidence of positive charges. As for the negative values, it was the presence of negative incompatible charges. It was noted that solutions number (NT4, NT6, NT7, NT8 NT3,) are nano-solutions prepared in the first and in the second way, that the value of The graph

of Zeta Potential (Fig. 19) is, respectively, 0.9 mv, -4.9 mv, -17.8mv, -25.1mv, -43.6 mv)) It is noted that the mv values are negative and very few, which means that no agglomeration occurs in the nanomaterial.

Antibacterial assays for nickel oxide nanoparticles

It was noted from the results in Table No. (2), the effect of nickel oxide solutions prepared in the first method NT4 of nano solutions has little effectiveness when they are at high concentrations of 100%M and have no effectiveness at dilute concentrations (25,50, 75) %M on the bacterial growth of Ps. aeruginosa and S. aureus, E. coli. As for the second method, the solutions (NT3,NT5, NT6, NT7, NT8) is NT6 solution, which is saffron extract with nickel nitrate, while NT5 and nickel chloride with saffron had an effect in concentrations (100, 75). M% and it was not effective on inhibiting bacterial growth at concentrations lower than that, NT7 solution which is nickel chloride with turmeric as well as NT8 as a solution of nickel chloride with ginger. As for the NT3 solution of nickel chloride with the extract of the plant, it was noted that the solution was effective in inhibiting St. aureus at a concentration of (100%M) while it was effective on Ps. aeruginosa at concentrations (100, 75, 50) M%. By comparing these results with the results of Table (8), it is noted that the effect of cobalt nitrate solutions with the extract of the aloe vera plant NT2 was the most significant inhibitory effect on the bacterial growth of Ps. aeruginosa and St. aeruginosa aureus. The aloe vera extract had an inhibitory effect on bacterial growth. aureus and this applies to what was reached (Al-Sharifi, 2018).

It is also noted that aloe vera extract had an effect on inhibiting bacteria on the growth of bacteria Ps. Aeruginosa (Jirátová et al., 2019). From the rates of diameters of inhibition, we find that the effect on Ps.aeruginosa, S. aureus was more than the effect on other species, where the average diameters of bacterial inhibition of the four plant extracts by the second method were (0.0,0.0,8,14,18,22,0.0. 8,9, 22,0.0,0.0,0.0,8,24,28,0.0,23,25,35). As for the study plant Cinnamomum verum, the average diameters of the inhibition areas were 0.0,0.0,0.0,60, 12,12,20) as its effect was the lowest compared to other extracts, but the inhibition effect of S.aureus bacteria was the average of 60 mm, which is the largest in the high concentrations of the extract with nickel chloride and even more effective than the plant extract Aloe vera L with cobalt nitrate as shown in Figure No. (1). (20). This is identical to what was found by Maruthamuthu and Ramanathan (2016)and has less effect on the negative bacteria Ps. aeruginosa, and the reason for this may be due to the nature of the bacterial cell wall as it contains bacteria Gram-negative layer of the outer membrane (Outer membrane) makes it less permeable to substances compared to gram-positive bacteria and this is what was found in the study (Sokrab, 2010) to Ps. aeruginosa in terms of response.

Table 2
Shows the effect of different concentrations of nanomaterials in the first and second methods of nickel oxide on inhibiting bacterial growth

How to prepare	How to prepare	plant name	Concentrations	The length of the	The length of the inhibiting	The length of

the solution	the solution		M%	inhibiting area is mm Pseudomonas aerogenos	area is mm Staphylococcus aureus	the inhibiting area is mm E.coli
The first method	The first method	NT4: nickel nitrate with sodium hydroxide	25	0.0	0.0	0.0
			50	0.0	0.0	0.0
			75	0.0	0.0	0.0
			100	0.0	32	0.0
The second method		NT3 Cinnamomum verum	25	0.0	0.0	0.0
			50	12	0.0	12
			75	12	0.0	12
			100	20	60	20
The second method		NT5 (Crocus sativus L	25	0.0	0.0	0.0
			50	0.0	0.0	0.0
			75	12	8	12
			100	23	30	23
The second method		NT6 (Crocus sativus L.	25	0.0	0.0	0.0
			50	0.0	0.0	0.0
			75	0.0	0.0	0.0
			100	0.0	8	0.0
The second method		NT7 Curcuma Longa	25	0.0	0.0	0.0
			50	8	14	8
			75	24	18	24
			100	28	22	28
The second method		NT8 Zingiber officinale	25	0.0	0.0	0.0
			50	23	8	23
			75	25	9	25
			100	35	22	35

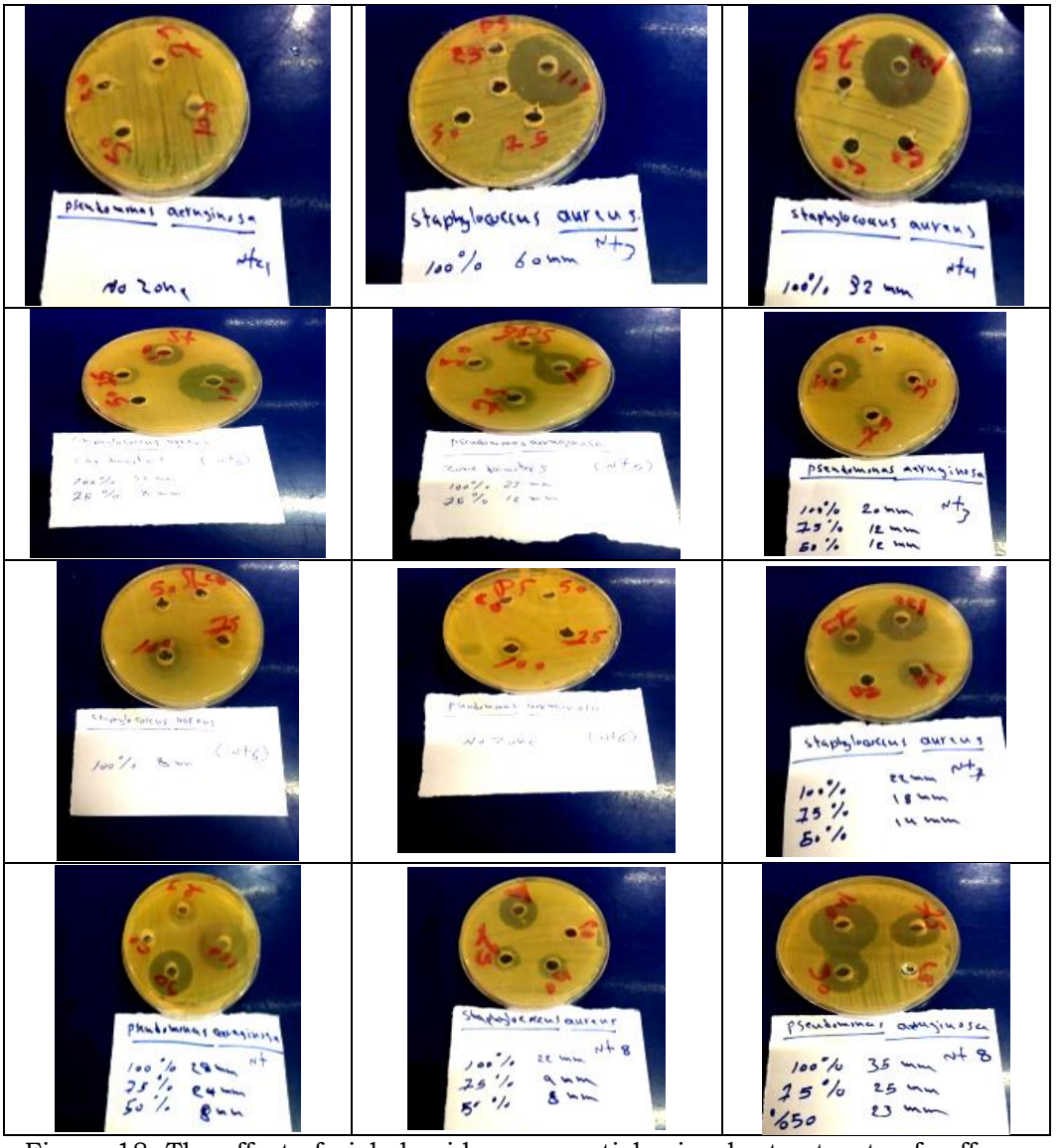

Figure 18. The effect of nickel oxide nanoparticles in plant extracts of saffron, turmeric, sage and ginger with nickel chloride on bacterial growth. Areas of inhibition on culture media using NT3, NT7 NT6, NT5, NT4, NT8 types of bacteria measured |-- | mm The numbers refer to the concentrations used. 20 mm = 1cm.

S = *S. auraus* , Ps = *Ps. aeruginosa* 1 =100 M , 2 =75 M 3= 50 M , 4 = Control

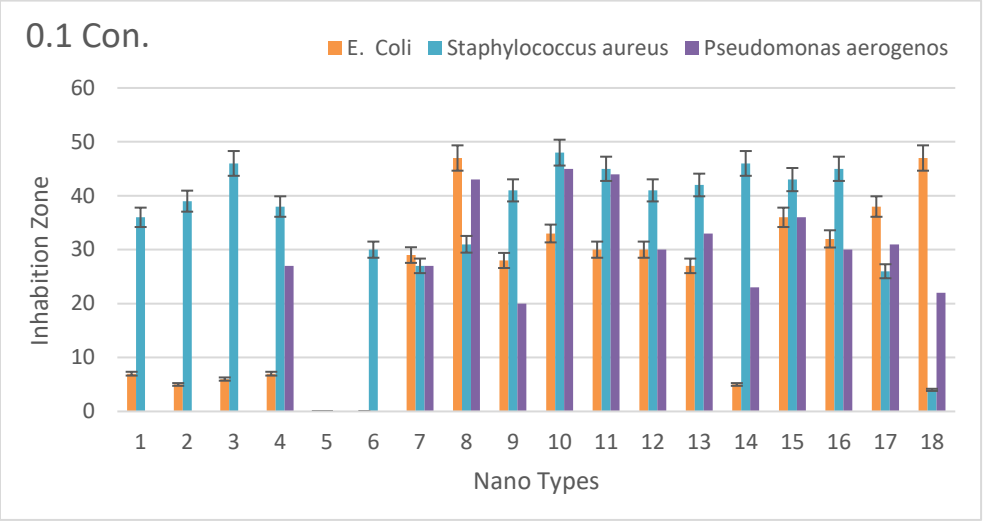

Figure 20. The graph shows the effect of different concentrations of nanomaterials in the first and second methods of nickel oxide on inhibiting bacterial growth using 0.1M% concentration of the solutions on S. auraus, Ps. aeruginosa, E. coli

Table 3
Shows the percentage of nanoparticle concentration in the first and second method and its effect on fungal growth

method	Plant name	concentrations%	The length of the diameter of the inhibiting area mm Candida albicans	The length of the diameter of the inhibiting area mm Trichophyton mentagrophytes
first method	NT4 :Nickel Nitrate + Sodium Hydroxide	0.0	0.0	0.0
		50	0.0	There is no fungal growth
		75	0.0	There is no fungal growth
		100	16	There is no fungal growth
The second method	Curcuma longa	0.0	0.0	0.0
		50	8	There is no fungal growth
		75	9	There is no fungal growth
		100	10	There is no fungal growth
The second method	Zingiber officinale	0.0	0.0	0.0
		50	0.0	There is no fungal growth
		75	10	There is no fungal growth
		100	23	There is no fungal growth
	Cinnamomum verum	0.0	0.0	0.0
		50	0.0	There is no fungal growth
		75	14	There is no fungal growth
		100	35	There is no fungal growth

The table shows that there is no growth and 100% inhibition of the fungus Trichphytone metagrophytes And that the nanomaterial had a great effect on inhibiting the growth of Candida albicans. Figure (10) shows the results of the cultivation of the fungus fungus using different concentrations of nano solutions.

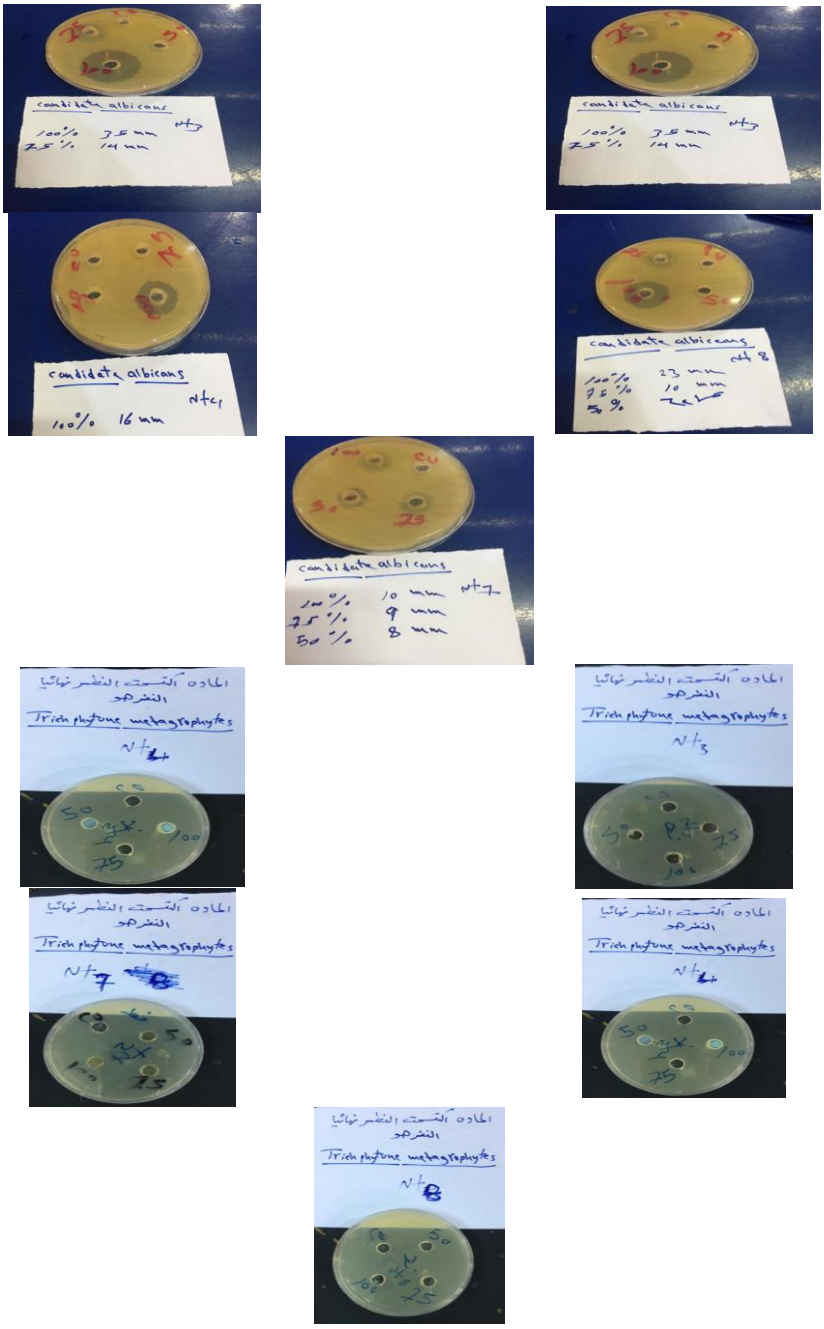

Figure 20. Shows the results of cultivation of Trichophytone metagrophytes using different concentrations of nano-solutions. Absence of Trichophyton mentagrophytes

The results show the effect of nickel oxide solutions on the growth of fungi, which have a significant inhibitory effect, as it shows the absence of fungal growth Trichophyton mentagrophytes and that the nanomaterial also had an effect on the inhibition of fungal growth Candida albicans with a diameter of 13,10.23,35 mm respectively at a concentration of 100 %.

Conclusion

It was found that nickel oxide prepared by the second method, Green synthesis nanoparticles by plant extract, is more efficient than the artificial roads nanoparticle in inhibiting isolates of S.aureus, E.coli and Ps.aeruginosa bacteria. It is more inhibited than Gram-negative bacteria Ps.aeruginosa. The plant extracts of nickel chloride with ginger had the most effect on the growth inhibition of Ps. aeruginosa bacteria. While it was highly effective in inhibiting the growth of Trichophyton mentagrophytes, Candida albicans.

Recommendations

The study recommends conducting chemical and technical studies of the active chemical components of nanomaterials for use in medical and therapeutic purposes. It also recommends using the GCMS examination of solutions to test the chemical content and applying the study of the possibility of using these extracts against pathogens in vivo Invivo, especially for other non-dermatological therapeutic uses of these extracts.

References

Ahmed, F. Y., Aly, U. F., Abd El-Baky, R. M., & Waly, N. G. (2020). Comparative study of antibacterial effects of titanium dioxide nanoparticles alone and in combination with antibiotics on mdr pseudomonas aeruginosa strains. International Journal of Nanomedicine, 15, 3393.

Al-Ani, Z. S., & Al-Qattan, M. M. D. (2017). Effect of boiled cinnamon extract on the blood picture and leptin hormone in New Zealand white rabbits infected with the disease.

Alcivar, M. S. G., Pérez, A. V., Gilert, B. I. C., & Gámez, M. R. (2017). Zeolite in wastewater decontamination as a local development solution. International Journal of Life Sciences, 1(3), 1–13. https://doi.org/10.21744/ijls.v1i3.52

AL-Hilli, F. (2000). Study of Antimicrobial effect of leaves extract from Callistemoncitrinuson Pseudomonas aeruginosa isolated from patients. M. Sc. Thesis, Coll. Sci., Univ. AL-Mustansiriya,

Al-Nashi, A. A.-R., & Al-Mansoori, R. W. H. (2017). Investigation of the phenotypic and molecular pattern of virulence factors of Staphylococcus bacteria. Staphylococcus spp, hemolyzed and isolated from urinary tract infections in Al-Diwaniyah. University of Al-Qadisiyah: College of Education

Al-Salmi, B. T. S. (2014). Study of some factors in the production of coagulase from locally isolated Staphylococci. University of Karbala,

Alteras, I., Aryeli, G., & Feuerman, E. (1980). The prevalence of pathogentic and potentially pathogenic fungi on the apparently healthy skin of patients with neoplastic diseases. Mycopathologia, 71(2), 85-87.

Archana, D., Nandish, M., Savalagi, V., & Alagawadi, A. (2013). Characterization of potassium solubilizing bacteria (KSB) from rhizosphere soil. Bioinfolet-A Quarterly Journal of Life Sciences, 10(1b), 248-257.

Bardají, D. K. R., da Silva, J. J. M., Bianchi, T. C., de Souza Eugênio, D., de Oliveira, P. F., Leandro, L. F., . . . Tavares, D. C. (2016). Copaifera reticulata oleoresin: chemical characterization and antibacterial properties against oral pathogens. Anaerobe, 40, 18-27.

Bassetti, M., Vena, A., Croxatto, A., Righi, E., & Guery, B. (2018). How to manage Pseudomonas aeruginosa infections. Drugs in context, 7.

Behzadi, P., Baráth, Z., & Gajdács, M. (2021). It's not easy being green: a narrative review on the microbiology, virulence and therapeutic prospects of multidrug-resistant Pseudomonas aeruginosa. Antibiotics, 10(1), 42.

Cianci, P., Slade Jr, J. B., Sato, R. M., & Faulkner, J. (2013). Adjunctive hyperbaric oxygen therapy in the treatment of thermal burns. Undersea & hyperbaric medicine: journal of the Undersea and Hyperbaric Medical Society, Inc, 40(1), 89-108.

Collee, J., Fraser, A., Marmion, B., & Simmons, A. (1996). Practical medical microbiology. 14 [sup] th ed. New York: Churchill Livingstone.

Eirmis, M. (1980). Laboratory handbook of medical mycology: Elsevier.

Emmons, S. W. (1974). Bacteriophage lambda derivatives carrying two copies of the cohesive end site. Journal of molecular biology, 83(4), 511-525.

Enders, A. A., North, N. M., Fensore, C. M., Velez-Alvarez, J., & Allen, H. C. (2021). Functional group identification for ftir spectra using image-based machine learning models. Analytical Chemistry, 93(28), 9711-9718.

Feliciano Guzmán, J. M. (2016). Frecuencia y susceptibilidad antifúngica de candida spp aislados en un hospital pediátrico del estado de Chiapas, México. Universidad de Ciencias y Artes de Chiapas,

Jalill, A., Raghad, D., Nuaman, R. S., & Abd, A. N. (2016). Biological synthesis of Titanium Dioxide nanoparticles by Curcuma longa plant extract and study its biological properties. World Scientific News, 49(2), 204-222.

Jawetz, E., & Melnick, J. (1980). Adelberg. EA. Review of Medical Microbiology, 186-191.

Jawetz, E., Adelberg, E. A., & Melnick, J. (1987). Microbiología médica.

Jirátová, K., Perekrestov, R., Dvořáková, M., Balabánová, J., Topka, P., Koštejn, M., . . . Kovanda, F. (2019). Cobalt oxide catalysts in the form of thin films prepared by magnetron sputtering on stainless-steel meshes: performance in ethanol oxidation. Catalysts, 9(10), 806.

Maruthamuthu, R., & Ramanathan, K. (2016). Phytochemical analysis of bark extract of Cinnamomum verum a medicinal herb used for the treatment of coronary heart disease in malayali tribes. International Journal of Pharmacognosy and Phytochemical Research, 8, 1218-1222.

Negi, M., Tsuboi, R., Matsui, T., & Ogawa, H. (1984). Isolation and characterization of proteinase from Candida albicans: substrate specificity. Journal of investigative dermatology, 83(1), 32-36.

Pal, S. L., Jana, U., Manna, P. K., Mohanta, G. P., & Manavalan, R. (2011). Nanoparticle: An overview of preparation and characterization. Journal of applied pharmaceutical science(Issue), 228-234.

Rahman, F., & Noor, R. (2012). Prevalence of pathogenic bacteria in common salad vegetables of Dhaka Metropolis. Bangladesh Journal of Botany, 41(2), 159-162.

Rusli, D., Ariani, D. N., Nurmina, N., & Rinaldi, R. (2021). Influence of exposure to children's movies on television on theory-of- mind acquisition in preschoolers. International Journal of Health & Medical Sciences, 4(1), 44-49. https://doi.org/10.31295/ijhms.v4n1.650

Seabra, A. B., & Durán, N. (2015). Nanotoxicology of metal oxide nanoparticles. Metals, 5(2), 934-975.

Sokrab, T.-E. O. (2010). See discussions, stats, and author profiles for this publication at: https://www. researchgate. net/publication/45459776 Hypothalamic hamartoma presenting with gelastic seizures, generalized convulsions, and ictal psychosis.

SOLL, D. R., & BEDELL, G. W. (1978). Bud formation and the inducibility of pseudo-mycelium outgrowth during release from stationary phase in Candida albicans. Microbiology, 108(2), 173-180.

Suryasa, I. W., Rodríguez-Gámez, M., & Koldoris, T. (2021). Get vaccinated when it is your turn and follow the local guidelines. *International Journal of Health Sciences*, *5*(3), x-xv. https://doi.org/10.53730/ijhs.v5n3.2938